

# Shiba multiplets due to Mn impurities in MgB<sub>2</sub>

Cătălin Pașcu Moca<sup>1,2,4</sup>, Gergely Zaránd<sup>1,3,4</sup>, Eugene Demler<sup>1,3</sup> and Boldizsár Jankó<sup>1,2</sup>

<sup>1</sup>Materials Science Division, Argonne National Laboratory,  
9700 South Cass Avenue, Argonne, Illinois 60439

<sup>2</sup>Department of Physics, University of Notre Dame, Notre Dame, Indiana, 46556

<sup>3</sup>Lyman Physics Laboratory, Harvard University, Cambridge MA

<sup>4</sup>Budapest University of Technology and Economics, H-1521 Budapest, Hungary

(Dated: November 20, 2018)

We study the effect of magnetic Mn ions on the two-band superconductor MgB<sub>2</sub>, and compute both the total and spin resolved scanning tunneling spectrum in the vicinity of the magnetic impurity. We show that when the internal structure of the Mn ion's *d*-shell is taken into account, multiple Shiba states appear in the spectrum. These multiplets were missed by previous calculations based on simplistic models, and their presence could alter significantly the overall interpretation of local tunneling spectra for a wide range of superconducting hosts and magnetic impurities.

PACS numbers: 75.30.Hx; 11.10.St; 74.25.Jb

The interaction between a single magnetic impurity and the superconducting host reveals fundamental properties of both the magnetic ion and the host material. This interaction was first studied theoretically, within the framework of BCS superconductivity. During the late sixties Shiba [1] showed that a magnetic impurity pulls down from the continuum states a pair of bound states inside the superconducting gap. Indirect indication for the presence of finite spectral weight inside the gap of an impure superconductor could be inferred from global probes of the density of states. However, direct evidence for the existence of the so-called Shiba states requires an accurate measurement of the *local* density of states near the impurity. Such a measurement became available only recently by using high vacuum, low temperature scanning tunneling spectroscopy (STS). Yazdani and his coworkers imaged[2] the local density of states around Mn and Gd impurities deposited onto Nb single crystals. They found clear evidence for localized states in the vicinity of the magnetic impurities, in qualitative agreement with Shiba's original findings, and also with their own model calculation based on a non-selfconsistent solution to Bogoliubov-de Gennes equations. Quantitative discrepancies, however, are also clearly present, especially when comparing the width and spatial dependence of the resonances to theoretical expectations. The presence of magnetic impurity induced bound states in a superconductor was turned around and used, both theoretically[3, 4, 5] and experimentally[6], as an investigative tool to probe the unusual ground state of the cuprate superconductors.

In all the studies carried out so far, the direct comparison between theory and experiment is hampered by the fact that the theoretical approaches, following Shiba's original work, use only a simplified (predominantly classical) model to describe the magnetic impurity, and assume a single spin one-half electron channel that couples to the magnetic impurity. Furthermore, the coupling is

assumed to be in the s-wave channel, and spin-orbit coupling is generally ignored. In reality, magnetic impurities usually have a much more complicated internal structure [20]: The magnetic moments are usually due to low-lying and crystal-field split *d*- or *f*-levels with multiple occupancy. The aim of this paper is to demonstrate that this internal structure has an impact on the structure of the Shiba states, and only part of the physics is captured by the simplified model used before. In particular, *multiple channels* of charge carriers couple to the magnetic impurity through channel-dependent coupling. The combination of these ingredients generally lead to the appearance of *multiple* pairs of Shiba states. We compute the spatial and spin structure of the scanning tunneling microscopy (STM) spectra around the magnetic impurity and show that these states appear as distinct resonances inside the superconducting gap, and can be most clearly resolved in spin resolved STM spectra.

In the following we illustrate our results on the specific case of Mn-doped MgB<sub>2</sub>, but we wish to emphasize that much of our discussions carry over to other systems as well, and that our conclusions are rather general. There are several reasons to choose the Mn – MgB<sub>2</sub> system. First, in order to observe a Shiba state by scanning tunneling spectroscopy (STS), one needs a relatively large gap. MgB<sub>2</sub> is a perfect candidate in this respect since it is a conventional superconductor that has an unusually high critical temperature,  $T_c = 39$  K [7]. Second, MgB<sub>2</sub> has a hexagonal *AlB<sub>2</sub>*-type structure and a highly anisotropic band structure [8, 9]. As we shall see below, this leads to a clear separation of the multiple Shiba states. Finally, there is increasing experimental evidence from spectroscopic [10, 11, 12], photoemission [13] and transport [14] measurements that favor the presence of two different superconducting gaps in MgB<sub>2</sub>. It is therefore an interesting question, how the presence of these two gaps influences the structure of Shiba states. As mentioned above, MgB<sub>2</sub> crystallizes in the hexagonal

AlB<sub>2</sub>-type structure [8] in which the B<sup>-</sup> ions constitute graphite-like sheets in the form of honeycomb lattices separated by hexagonal layers of Mg ions. Band structure calculations [9] indicate that Mg is substantially ionized, and the bands at the Fermi level derive mainly from Boron *p* orbitals. Four of the six *p* bands cross the Fermi energy, and the Fermi surface consists of quasi-2D cylindrical sheets, due to B - *p*<sub>*x,y*</sub> orbitals, and a 3D tubular network (mostly originating from B - *p*<sub>*z*</sub> orbitals). It is believed that both structures participate in the formation of the superconducting state, though the gap is very different on the tubular network and on the cylindrical sheets.

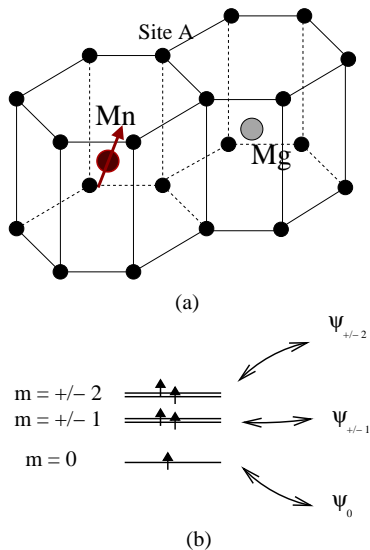


FIG. 1: Fig. a: Local environment of an Mn ion in MgB<sub>2</sub>. The Mn ion is located in a hexagonal cage. Fig. b: Level structure and crystal field splitting of the Mn<sup>2+</sup> core states.

We begin the quantitative analysis of the magnetic impurity problem by establishing how the Mn spins couple to the conduction electrons. The interaction part of the Hamiltonian depends on the specific location and electronic structure of the magnetic impurity considered. In what follows, we provide a detailed analysis for Mn impurities, which presumably substitute the Mg ions, and take an Mn<sup>2+</sup> configuration with a half-filled *d*-shell and a spin  $S = 5/2$  [21], though similar considerations hold for other types and positions of magnetic impurities. As shown in Fig. 1, the five-fold degeneracy of the *d*-states is lifted by the local hexagonal crystal field into three multiplets that we can label by the original angular momentum quantum numbers  $m$  of the *d*-states  $|m\rangle$ . Each of these states is occupied by a single electron, and hybridizes through a hybridization  $V_m$  with a specific local combination of *p*-states,  $\psi_m$ , that we constructed explicitly in the framework of a simple tight binding description of the *p*-bands [18]. The  $\psi_m$ 's transform the same

way under the hexagonal point group as the  $|m\rangle$ 's. Incorporating the local Hund's rule coupling and Coulomb interaction and the *d*-states and integrating out virtual charge fluctuations to them we arrive at the following exchange Hamiltonian:

$$H_{\text{int}} = \frac{1}{2} \sum_{m=-2}^2 J_m \mathbf{S} (\psi_m^\dagger \boldsymbol{\sigma} \psi_m), \quad (1)$$

where the exchange couplings satisfy  $J_m = J_{-m} \sim V_m^2/\Delta E$ , with  $\Delta E$  the characteristic energy of charge fluctuations, and the  $\boldsymbol{\sigma}$ 's denote the Pauli matrices. Note that Eq. (1) must conserve  $m$  by symmetry, and therefore *five* independent channels couple simultaneously to the impurity. This is the ultimate reason for the appearance of multiple Shiba states.

To analyze the Shiba states in detail, we described the superconducting state of MgB<sub>2</sub> by the following non-interacting BCS Hamiltonian:

$$H_0 = \sum_{\alpha, \mathbf{k}, \sigma} \varepsilon_{\mathbf{k}, \alpha} c_{\mathbf{k}\alpha\sigma}^\dagger c_{\mathbf{k}\alpha\sigma} + \sum_{\alpha, \mathbf{k}} \Delta_\alpha (c_{-\mathbf{k}\alpha\downarrow}^\dagger c_{\mathbf{k}\alpha\uparrow}^\dagger + \text{h.c.}).$$

Here  $c_{\mathbf{k}\alpha\sigma}^\dagger$  creates an electron with momentum  $\mathbf{k}$ , spin  $\sigma$ , energy  $\varepsilon_{\mathbf{k}, \alpha}$ , and wave function  $\phi_{\alpha, \mathbf{k}}$  in one of the four bands that cross the Fermi energy ( $\alpha = 1 \dots 4$ ). The kinetic energies  $\varepsilon_{\mathbf{k}, \alpha}$  and the corresponding wave functions have been constructed using a simple tight binding model, which has proved quite accurate in the vicinity of the Fermi surface [18]. We assume further that the superconducting gaps take two different values in the *p*<sub>*x,y*</sub> and *p*<sub>*z*</sub> bands  $\Delta_{xy} \approx 7.5$  meV and  $\Delta_z \approx 2.5$  meV.

As a next step, we express the interaction part Eq. (1) in terms of the operators  $c_{\mathbf{k}\alpha\sigma}^\dagger$  and re-express the Hamiltonian in terms of Nambu spinors [19]  $\Phi_{\mathbf{k}, \alpha} \equiv \{c_{\mathbf{k}, \alpha, \uparrow}, c_{\mathbf{k}, \alpha, \downarrow}, -c_{-\mathbf{k}, \alpha, \downarrow}^\dagger, c_{-\mathbf{k}, \alpha, \uparrow}^\dagger\}$  to obtain

$$H = \sum_{\mathbf{k}, \alpha} \Phi_{\mathbf{k}, \alpha}^\dagger (\varepsilon_{\mathbf{k}, \alpha} \tau^z + \Delta_\alpha \tau^x) \Phi_{\mathbf{k}, \alpha} \quad (2) \\ + \sum_{\substack{\mathbf{k}, \mathbf{k}' \\ \alpha, \beta, m}} \frac{1}{2} J_m^{\alpha\beta} f_{m, \alpha}^*(\mathbf{k}) f_{m, \beta}(\mathbf{k}') \Phi_{\mathbf{k}, \alpha}^\dagger \boldsymbol{\sigma} \cdot \mathbf{S} \Phi_{\mathbf{k}', \beta}.$$

The  $\tau^i$ 's here denote Pauli matrices acting in the pseudospin (charge) index of the Nambu spinor. In course of the derivation we made use of time reversal symmetry and doubled the Hilbert space so that the components of the Nambu spinors in Eq. 2 must be considered as independent variables. The form factors  $f_{m, \alpha}(\mathbf{k})$  are normalized such that they satisfy the orthogonality relation on the Fermi surface  $S_\alpha$ :

$$\int_{S_\alpha} d^2 \mathbf{k} f_{m, \alpha}(\mathbf{k}) f_{m', \alpha}^*(\mathbf{k}) = \delta_{m, m'} S_\alpha. \quad (3)$$

We determined both the couplings  $J_m^{\alpha\beta}$  and the form factors within the tight binding model of MgB<sub>2</sub> [18]: In

this approximation – apart from an overall prefactor in  $J_m^{\alpha\beta}$  – they uniquely depend on the crystal structure of  $\text{MgB}_2$ . The couplings  $J_m^{\alpha\beta}$  in Eq. 2 approximately satisfy  $J_m^{\alpha\beta} \approx (J_m^{\alpha\alpha} J_m^{\beta\beta})^{1/2}$  and are equal in channels  $\pm m$  by symmetry. In the rest of the paper, we neglect quantum fluctuations of the Mn spin and treat  $S$  as a classical variable. In this limit we can solve the impurity problem exactly. To determine the STM spectrum we first compute the Nambu Green's function in the presence of the impurity:

$$G(\alpha, \beta, \mathbf{k}, \mathbf{k}', \omega) = \delta_{\mathbf{k}, \mathbf{k}'} \delta_{\alpha, \beta} G_\alpha^{(0)}(\mathbf{k}, \omega) + G_\alpha^{(0)}(\mathbf{k}, \omega) \sum_m \frac{1}{\Omega} f_{m, \alpha}^*(\mathbf{k}) T_m^{\alpha, \beta}(\omega) f_{m, \beta}(\mathbf{k}') G_\beta^{(0)}(\mathbf{k}', \omega), \quad (4)$$

where  $G_\alpha^{(0)}(\mathbf{k}, \omega) = (\omega - \varepsilon_{\alpha, \mathbf{k}} \tau^z - \Delta_\alpha \tau^x)^{-1}$  denotes the non-interacting momentum space Nambu Green's function in band  $\alpha$ . Eq. (3) guarantees that the quantum number  $m$  is conserved and thus the T-matrix  $T^{(m)}$  can be computed independently for each channel  $m$ . The computation simplifies further because  $G_\alpha^{(0)}$  depends on  $\mathbf{k}$  only through the energy  $\varepsilon_{\alpha, \mathbf{k}}$ . As a result, we can express  $T_m^{\alpha, \beta}$  simply as

$$\mathbf{T}_m(\omega) = \mathbf{J}_m \mathbf{S} \sigma / 2 [1 - \mathbf{F}(\omega) \mathbf{J}_m \mathbf{S} \sigma / 2]^{-1}, \quad (5)$$

where we introduced a matrix notation in the band indices,  $J_m^{\alpha\beta} \rightarrow \mathbf{J}_m$ ,  $T_m^{\alpha, \beta} \rightarrow \mathbf{T}_m$ . The matrix  $F_{\alpha, \beta}(\omega) = \delta_{\alpha, \beta} F_\alpha(\omega) \rightarrow \mathbf{F}$  in Eq. 5 simply denotes the local Nambu propagator:

$$F_\alpha(\omega) = \int_{-\infty}^{\infty} d\varepsilon \varrho_\alpha \frac{1}{\omega - \varepsilon \tau^z - \Delta_\alpha \tau^x}, \quad (6)$$

with  $\varrho_\alpha$  the density of states at the Fermi energy in band  $\alpha$ . For  $|\omega| < \Delta_\alpha$  the function  $F_\alpha(\omega)$  has only real parts and simplifies to  $F_\alpha(\omega) = -\pi \varrho_\alpha (\omega + \Delta_\alpha \tau^x) / (\Delta_\alpha^2 - \omega^2)^{-1/2}$ , while for  $|\omega| > \Delta_\alpha$  it is purely imaginary.

Impurity bound states and resonances can be identified from the pole structure of the T-matrix: True bound states correspond to zeros of the determinants  $\det\{\mathbf{T}_m^{-1}(\omega)\}$  on the real axis, and must satisfy  $|\omega| < \Delta_\alpha$  for all bands. Zeros in the vicinity of the real axis, on the other hand, correspond to resonances. We found that each of the five channels generates a pair of bound states, two of which are doubly degenerate by symmetry.

Let us first discuss the case of two bands only. There the calculations further simplify and the energies  $E$  of the bound states satisfy the following implicit equations:

$$(1 - g_m^{11} \alpha_1(\pm E))(1 - g_m^{22} \alpha_2(\pm E)) = (g_m^{12})^2 \alpha_1(\pm E) \alpha_2(\pm E), \quad (7)$$

with  $g_m^{\alpha\beta} \equiv \pi S \sqrt{\varrho_\alpha \varrho_\beta} J_m^{\alpha\beta} / 2$  the dimensionless couplings in channel  $m$ , and

$$\alpha_\alpha(\omega) = \left( \frac{\Delta_\alpha + \omega}{\Delta_\alpha - \omega} \right)^{1/2}.$$

In the absence of inter-band coupling,  $g^{12} = 0$  Eq. (7) would have two independent solutions for each  $m$ , and the presence of the second superconducting gap would double the number of Shiba states. For small  $g^{12}$ 's the bound states with energies  $\Delta_z < |E| < \Delta_{xy}$  evolve into resonances due to mixing with the continuum. We have in fact shown that in reality  $g^{12}$  is large. Consequently, the naive expectation mentioned above - based solely on the straightforward extension of Shiba's result for two bands - is not correct. Using the approximate relation for  $(g_m^{12})^2 \approx g_m^{11} g_m^{22}$ , we obtain that

$$g_m^{11} \alpha_1(\pm E) + g_m^{22} \alpha_2(\pm E) = 1, \quad (8)$$

which has only one pair of solutions for each  $m$ . Exchange coupling between the two bands thus removes half of the resonances, and the number of Shiba states is not increased due to the presence of the second gap in this case. We thus obtain altogether *five* pairs of Shiba states corresponding to the five channels, but two of them are two-fold degenerate because of the symmetry  $J_m^{\alpha\beta} = J_{-m}^{\alpha\beta}$ .

We are most interested in the total and spin resolved tunneling density of states in the vicinity of the Mn sites, which are directly measured by conventional and spin polarized STM techniques[22], respectively, and are related to the local Nambu Green's function  $G(\mathbf{R}, p_\alpha, \omega)$  at site  $\mathbf{R}$  and orbital  $p_\alpha$  ( $\alpha = x, y, z$ ) as

$$\varrho_{c, \alpha}(\omega) = -\frac{1}{2\pi} \text{ImTr} \left\{ G(\mathbf{R}, p_\alpha, \omega) \frac{1 + \tau_z}{2} \right\}, \quad (9)$$

$$\varrho_{s, \alpha}(\omega) = -\frac{1}{2\pi} \text{ImTr} \left\{ G(\mathbf{R}, p_\alpha, \omega) \boldsymbol{\sigma} \mathbf{n} \frac{1 + \tau_z}{2} \right\} \quad (10)$$

with  $\mathbf{n}$  a unit vector pointing in the direction of the Mn spin. These can be computed easily from (4) in terms of the electronic wave functions  $\phi_{\alpha, \mathbf{k}}$  [18].

To obtain a quantitative estimate for the STM spectra we performed a lengthy, but straightforward tight-binding calculation to determine numerically the form factors, the exchange couplings and the electronic wave functions above in various geometries. In particular, we generalized the discussions above for the case of a semi-infinite half plane and computed the STM spectra as a function of the Mn positions [18]. In these calculations we assumed that the value of the order parameter does not depend on the distance from the surface.

In Fig. 2 we show the density of states for the case of a half-infinite sample for various values of the dimensionless exchange coupling,  $g \equiv \frac{1}{5} \sum_{m, \alpha} \varrho_\alpha J_m^{\alpha\alpha}$ , with  $\varrho_\alpha$  the density of states in band  $\alpha$  per one spin direction at the Fermi energy. We assumed that  $\text{MgB}_2$  is cleaved along a Boron sheet and that the Mn ion sits right below this Boron layer. In the STM experiment one presumably tunnels into the  $p_z$  orbitals oriented perpendicularly to the Boron plane. Therefore we plotted the DOS that corresponds to a local  $p_z$  orbital at position A. For generic values of the exchange coupling usually

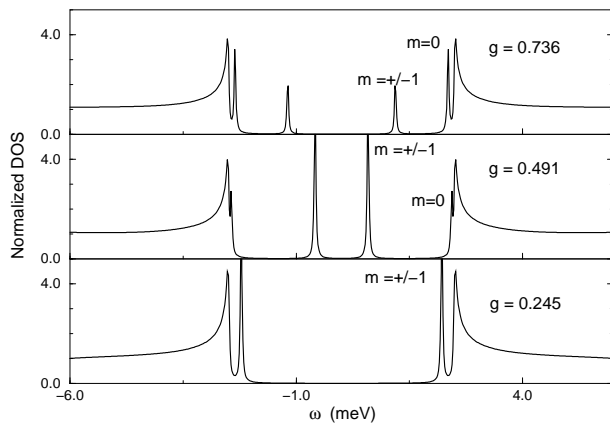


FIG. 2: Normalized density of states for site A as function of frequency for different values of  $g$ .

two well-separated pairs of resonances can be observed, corresponding to the  $m = \pm 1$  and  $m = 0$  channels. The exchange couplings in channels  $m = \pm 2$  are much smaller than those in channels  $m = \pm 1$  and  $m = 0$ , therefore the bound state appears at the superconducting coherence peak. The wave functions of the Shiba states and thus the amplitudes of the corresponding resonances in the spectrum depend a lot on the tunneling position[18]. Moreover, as we show in Fig. 3, the Shiba states are strongly spin-polarized. Therefore, even if a peak happens to be close to the BCS coherence peaks, a spin-polarized STM can distinguish the Shiba state from the coherence peak. Thus, spin-polarized STM would provide a perfect tool to identify these multiple Shiba states.

The presence of spin-orbit coupling should not influence these results: Since the  $\pm m$   $d$ -levels form time reversed pairs, the symmetry  $J_m = J_{-m}$  should hold even if we take spin-orbit coupling into account. We conjecture therefore that the Shiba states remain degenerate even in the presence of spin-orbit coupling.

Finally, let us shortly discuss how these results generalize for other compounds. Possible crystal field structures in other cases and the corresponding exchange Hamiltonians have been discussed for various point symmetries in the seminal paper of Nozières and Blandin [20]. Though the form of the exchange Hamiltonian depends a lot on the specific material, in many cases, similar to Mn-doped  $\text{MgB}_2$ , several channels of conduction electrons couple to the local impurity degrees of freedom, and result in multiple Shiba states. Thus the appearance of multiple Shiba states seems to be a rather general phenomenon.

In conclusion, we have shown that a magnetic impurity generally induces multiple Shiba states in the electronic structure of  $\text{MgB}_2$ . In particular for Mn we found five pairs of Shiba states in the gap, two of which were two-fold degenerate. We computed both conventional and spin-resolved STM spectra near the impurity site and

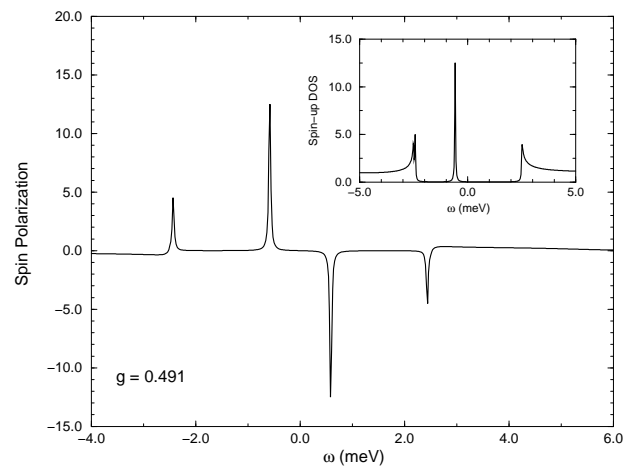


FIG. 3: Spin polarization and spin resolved density of states (inset) for site A and  $g = 0.491$ .

showed that these states can be clearly resolved by both methods. Similar multiple Shiba states should appear in other superconductors due to the internal structure of the magnetic impurity.

*Acknowledgments* We are grateful to Drs. Dan Agterberg, George Crabtree, J.C. Seamus Davis, Maria Iavarone, Goran Karapetrov, Igor Mazin, Kaori Tanaka, Ali Yazdani, and John Zasadzinski for useful discussions. This work was supported by the U.S. Dept. of Energy, Office of Science, under Contract No. W-31-109-ENG-38, Hungarian Grants No. OTKA F030041, T038162, the Bolyai foundation, and the EU “Spintronics” RTN. BJ was supported by NSF-NIRT award DMR02-10519 and the Alfred P. Sloan Foundation. ED was supported by US NSF grant DMR-0132874.

- 
- [1] H. Shiba, Prog. Theor. Phys. **40**, 435, (1968).
  - [2] A. Yazdani, B. A. Jones, C. P. Lutz, M. F. Crommie, D. M. Eigler Science **275**, 1767 (1997).
  - [3] D. Poilblanc, D. J. Scalapino, W. Hanke, Phys. Rev. Lett. **72**, 884-887 (1994); J. M. Byers, M. E. Flatt, D. J. Scalapino, Phys. Rev. Lett. **71**, 3363-3366 (1993).
  - [4] M. E. Flatté, D. E. Reynolds, Phys. Rev. **B 61**, 14810, (2000).
  - [5] A. V. Balatsky, M. I. Salkola, A. Rosergren, Phys. Rev. **B51**, 15547, (1995); M. I. Salkola, A. V. Balatsky, J. R. Schrieffer, *ibid.* **55**, 12648, (1997).
  - [6] S. H. Pan, E. W. Hudson, K. M. Lang, H. Eisaki, S. Uchida, J. C. Davis, Nature **403**, 746, (2000); E. W. Hudson, S. H. Pan, A. K. Gupta, K. W. Ng, J. C. Davis, Science, **285**, 88, (1999).
  - [7] J. Nagamatsu, N. Nakagawa, T. Muranaka, Y. Zenitani, J. Akimitsu, Nature **410**, 63, (2001).
  - [8] S. L. Bud’ko, G. Lapertot, C. Petrovic, C. E. Cunningham, N. Anderson, P. C. Canfield, Phys. Rev. Lett. **86**,

- 1877, (2001).
- [9] J. Kortus, I. I. Mazin, K. D. Belashchenko, V. P. Antropov, L. L. Boyer, Phys. Rev. Lett. **86**, 4656, (2001).
- [10] F. Giubileo, D. Roditchev, W. Sacks, R. Lamy, D.X. Thanh, J. Klein, Phys. Rev. Lett. **87**, 177008 (2001).
- [11] P. Szabo, P. Samuely, J. Kacmarcik, Th. Klein, J. Marcus, D. Fruchart, S. Miraglia, C. Marcenat, A.G.M. Jansen, Phys. Rev. Lett. **87**, 137005 (2001).
- [12] H. Schmidt, J. F. Zasadzinski, K. E. Gray, D. G. Hinks, Phys. Rev. **B** **63**, 220504, (2001).
- [13] S. Tsuda, T. Yokoya, T. Kiss, Y. Takano, K. Togano, H. Kitou, H. Ihara, S. Shin, [cond-mat/0104489](#).
- [14] Y. Wang, T. Plackowski, A. Junod, Physica **C**, **355**, 179, (2001).
- [15] S. L. Bud'ko, C. Petrovic, G. Lapertot, C. E. Cunningham, P. C. Canfield, M-H. Jung, A. H. Lacerda, [cond-mat/0102413](#).
- [16] H. Suhl, B. T. Matthias, L. R. Walker, Phys. Rev. Lett. **3**, 552, (1959).
- [17] F. Bouquet, Y. Wang, R. A. Fisher, D. G. Hinks, J. D. Jorgensen, A. Junod, N. E. Phillips, Europhys. Lett. **56**, 856 (2001).
- [18] C. P. Moca, G. Zaránd, E. Demler, B. Jankó, (unpublished).
- [19] With this definition Nambu spinors have nice transformation properties, which allows us to express the total Hamiltonian in an especially simple and transparent form. [See *e.g.* P. Coleman, E. Miranda, and A. Tsvelik, Phys. Rev. B **49**, 8955-8982 (1994).]
- [20] Nozières and Blandin. J Phys. Paris **41**, 193, (1980).
- [21] S. Xu, Y. Moritomo, K. Kato, A. Nakamura, J. Phys. Soc. Japan **70**, 1889, (2001).
- [22] S. Heinze, M. Bode, A. Kubetzka, O. Pietzsch, X. Nie, S. Bluger, R. Wiesendarger, Science **288**, 1805, (2000).